In *Solar Physics and Astrophysics at Interferometric Resolution*, L. Damé, T.D. Guyenne (Eds.), ESA SP-344, pp. 197-200 (1992).

POLARIMETRY WITH AN IMAGING FTS

J.O. STENFLO and S.K. SOLANKI

Institute of Astronomy, ETH-Zentrum, CH-8092 Zurich, Switzerland

ABSTRACT

The concept of an imaging FTS polarimeter based on piezoelastic modulation and direct demodulation in partially masked CCDs is outlined. To illustrate its principle the currently operational FTS polarimeter at the McMath telescope as well as the detection scheme of the ETH polarimeter, based on partially masked CCD cameras, are briefly described.

Keywords: Polarimetry — Fourier transform spectrometer (FTS) — Solar magnetic fields.

1. INTRODUCTION

The whole range of phenomena observed in solar UV spectra and images is directly or indirectly related to the solar magnetic field. The SIMURIS project would, therefore, be greatly enhanced by a simultaneous measurement of the photospheric magnetic field with an imaging FTS. The basics of the possible configuration of an imaging FTS polarimeter are described in the present contribution. The type of polarimeter described here is also easily applicable to SUN. However, as there will probably be problems with the photon flux in the UV, we envisage mainly applications in the visible.

The study of solar magnetism thrives on high spatial resolution observations. At each increase of the spatial resolution smaller and smaller magnetic structures have been discovered. Even with the best present spatial resolution the basic building blocks of the solar field, small magnetic flux tubes, are not spatially resolved. Since solar magnetism can be properly studied only in the polarized spectrum, simple white-light imaging gives very little information on the distribution and nature of most of the magnetic field. Filtergrams are also of only limited value. An imaging spectral polarimeter would give us the unique possibility of determining the true magnetic flux, magnetic field strength and inclination, thermal and velocity stratification in all three dimensions in the solar photosphere and possibly in the chromosphere.

At present no dedicated imaging spectral polarimeter exists or is under construction. Compared to other conceivable imaging spectro-polarimeters an FTS has some inherent advantages. For example, it has no spectral stray light and has a very clean and well defined spectral profile. The latter is particularly relevant for polarimetry since the Stokes V, Q and U profiles are easily distorted by winged and asymmetric spectral profiles (e.g. Solanki and Stenflo 1986). Having such an instrument above the earth's atmosphere is important, since it allows longer integration times without distortions due to variable seeing (i.e. characteristic time scales on the sun and not in the earth's atmosphere limit the duration of a single, successful high resolution measurement).

The introduction of an imaging FTS polarimeter will revolutionize solar magnetic field investigations, considering that polarimetric observations with a simple FTS (the McMath FTS polarimeter described in Sect. 2) already produced a breakthrough of our knowledge of the physical structure of solar magnetic features (e.g. Solanki 1987, Stenflo 1989).

2. PRESENT POLARIMETRIC SCHEME AT THE MCMATH FTS

The only existing FTS polarimeter is at the 1-m FTS (Brault 1978) of the McMath telescope. It has been designed by J.W. Harvey and used for explorations of the scattering polarization near the solar limb (Stenflo et al. 1983) and of the Zeeman effect for diagnostics of small-scale magnetic flux tubes (Stenflo et al. 1984, 1987). As many of its operating principles can be used for an imaging FTS polarimeter, we briefly outline how the scheme works.

So far the simultaneous recording of three Stokes parameters (I, Q, and V) has been implemented, but as the extension to four Stokes parameters is straightforward, we will here describe it as if Stokes U is also recorded. Piezoelastic modulation at frequencies of 20-40 kHz is used, so we will here assume that the incoming beam is modulated at the three frequencies ω_Q, ω_U, and ω_V, carrying the information on Q, U, and V.

The McMath FTS is sampled at a frequency of 2.5 kHz. The spectral intensities cause an amplitude modulation of the sampling signal, such that the wavelengths are mapped into audio frequencies. In ordinary operation (no under-sampling), the visible wavelengths are mapped into the range around 800–1000 Hz. The procedure is now to map the Stokes Q, U, and V spectra into

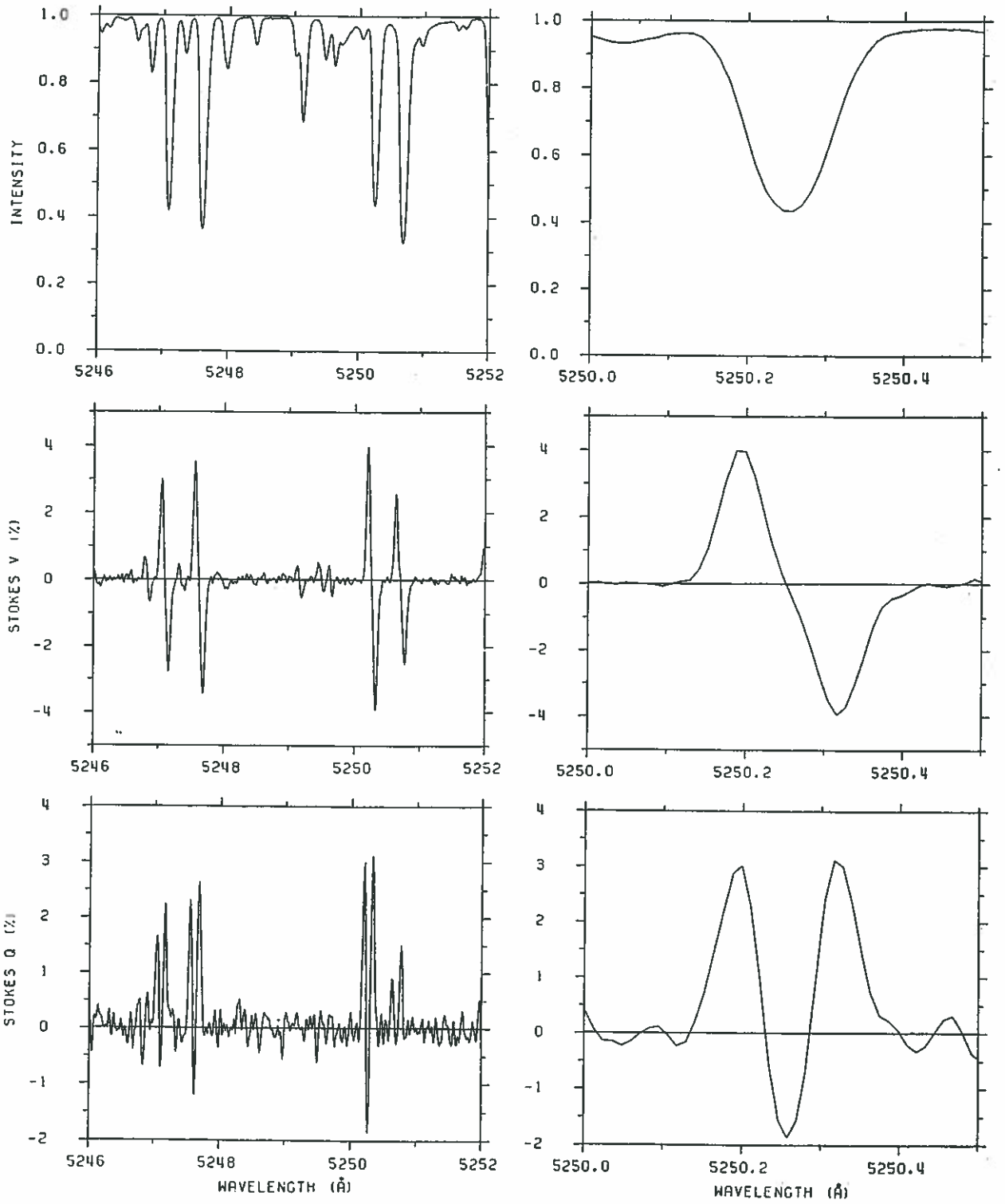

Fig. 1: From top to bottom Stokes I/I_c, V/I_c and Q/I_c vs. wavelength. The frames on the right show in greater detail one of the spectral lines present in the frames on the left.

separate free portions of the remaining frequency range (0–800 Hz) available to the A/D converter.

The convolution of the modulation frequencies with the audio frequencies generated by the sampling of the interferogram causes the Stokes Q, U, and V spectra to appear at frequencies $\omega_{Q,U,V}/2\pi \pm (800 - 1000)$ Hz. The signal is sent to three parallel lock–in amplifiers, which demodulate each of the three modulation frequencies, thereby essentially shifting $\omega_{Q,U,V}$ back to zero. To avoid that the Stokes Q, U, and V spectra fall on top of the Stokes I spectrum, they have to be frequency shifted (heterodyned) into three separate free frequency ranges. The heterodyning is done by mixing the three signals from the lock–in amplifiers with suitable frequencies derived from the FTS 2.5 kHz sampling pulses.

Like in ordinary photometric use, the FTS polarimeter can also be used with under–sampling in higher order aliases, to achieve increased time resolution. As the free spectral range then decreases, the spectral bandwidth has to be reduced accordingly with prefilters.

Short extracts of a Stokes I/I_c, V/I_c and Q/I_c spectrum (where I_c is the continuum intensity), measured with the McMath FTS polarimeter in a solar plage at $\mu = \cos\theta \approx 0.28$, are plotted in Fig. 1. The frames on the left show extracts centered on 5249

Å, while the frames on the right show a blow-up of the Fe I 5250.2 Å line. The complete observed spectrum covers approximately 1000 Å. Noise in I/I_c and V/I_c is approximately 4×10^{-4}, while the noise in Q/I_c is approximately $1\text{–}2 \times 10^{-3}$.

3. STOKES POLARIMETRY WITH 2–DIMENSIONAL DETECTOR ARRAYS IN AN IMAGING FTS

With the use of two-dimensional detector arrays, one can make use of the multiplexing potential of the FTS to record the spectra of many spatial points simultaneously, thereby obtaining images. The use of lock–in amplifiers to detect the modulated Stokes parameters as in the present McMath FTS is then not practical, since one would essentially need one set of lock–in amplifiers for each pixel. Also, the polarization modulation is too fast for sampling at the modulation rate.

A solution to this problem has been described by Stenflo and Povel (1985) and by Povel et al. (1990), whereby the lock–in amplifiers are replaced by optical demodulators, which demodulate the signal for all the pixels simultaneously. Behind the FTS exit focal plane the beam is first collimated, then split into three equal parts, each beam going to a demodulator for one of the frequencies ω_Q, ω_U, or ω_V. A first scheme for such a demodulator, which has been described in detail in Stenflo and Povel (1985), contains a piezoelastic modulator locked in frequency and phase to the modulation frequency that it is supposed to demodulate, and a Wollaston polarizing beam splitter, producing two output beams of orthogonal linear polarization, which are then re-imaged onto two separate arrays or onto two portions of the same array. (The additional phase switch described in the original paper is not needed.) The two images are now already demodulated, which means that the signals can be integrated in time over any periods long compared with the modulation period without loss of the polarization information. The Stokes Q, U, or V images are obtained simply as the difference between the two images produced by the Wollaston prisms, assuming that the pixel–to–pixel sensitivity variations have been fully corrected for (flat–fielding). While it is very difficult to generate an accurate photometric flat field, it is easy to generate a calibration field that is perfectly flat in the *degree of polarization*.

A considerably more elegant demodulation scheme has been described by Povel et al. (1990). The demodulation is done in the CCD itself by shifting the charges from light sensitive to insensitive areas on the chip and back again during a single modulation cycle. Each chip simultaneously stores two images in orthogonal polarization states. When one image is being exposed, the other resides in an unexposed storage region of the CCD. During the next half-period of the modulation the two images exchange places, and so forth. In this manner the signal on the detector may be integrated over many modulation cycles without losses. Also, there is no problem of matching different detector areas for two orthogonal polarizations, since both are detected by exactly the same pixels. Therefore, the degree of polarization Q/I, U/I, and V/I can be obtained in an unblemished form without any flat-fielding.

The second scheme (due to Povel et al. 1990) imposes two requirements on the CCDs:

1. There must be a zone on the CCD shielded from light where the two images can be stored alternately during the two modulation half cycles.

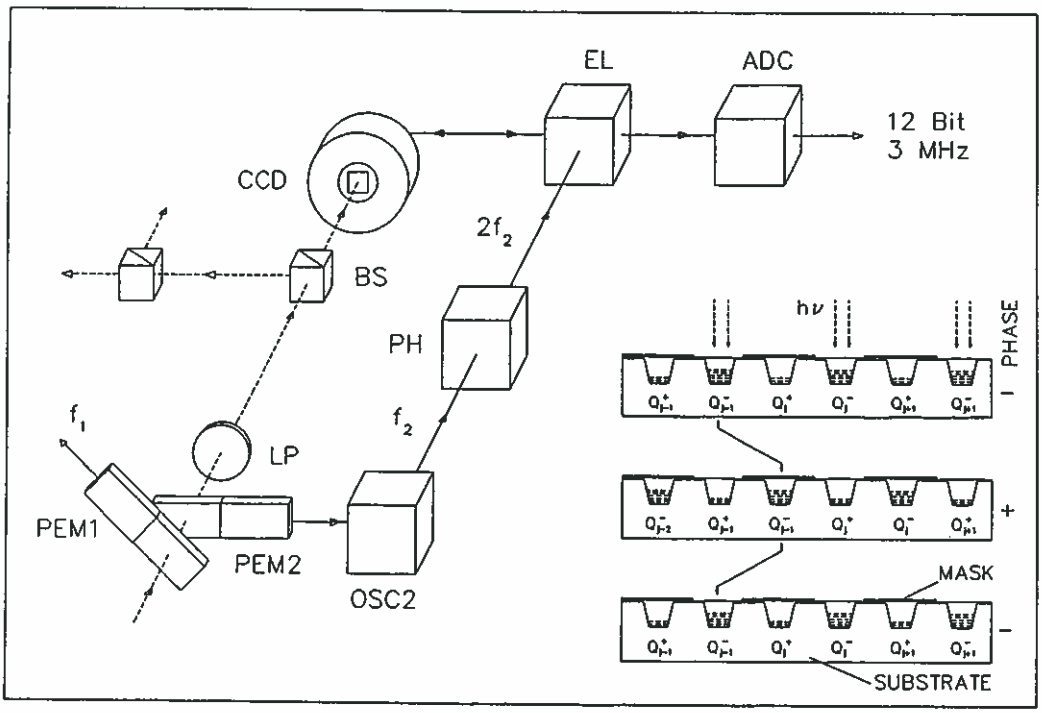

Fig. 2. Schematic representation of the current implementation of the ETH CCD-polarimeter (with a single CCD camera). The abbreviations have the following meanings: PEM = piezo-elastic modulator, LP = linear polarizer, BS = beam splitter, CCD = CCD camera, OSC = oscillator, PH = phase shifter (to align optical modulation and electronic demodulation), EL = electronics, ADC = A/D converter. The two beamsplitters send part of the light to other cameras (three cameras are needed to measure all four Stokes parameters simultaneously. Such a system is currently under construction). The inset shows the principle of demodulating directly in the CCD by transfering charges back and forth between neighbouring rows of the CCD during the oscillation cycle of the modulator. Adapted from Povel et al. (1991), courtesy of P. Povel.

2. The structure of the CCD must be such that the image charge can be moved back and forth between the storage and the light-sensitive zones on time-scales short compared to the modulation half-cycles.

A three–phase CCD satisfies the second requirement very well. In order to satisfy the first requirement, either a mask must be projected optically onto the CCD (Povel et al. 1990), or a mechanical mask must be fitted onto the CCD during production (Povel et al. 1991). The latter course is technically feasible, and such CCDs have been produced and integrated into a solar polarimeter at the ETH. The masks on the CCDs of the ETH polarimeter are chosen such as to cover every second row of pixels of the CCD. The CCD polarimeter of the ETH is schematically depicted in Fig. 2. The inset (lower right part) in that figure shows cross-sections through a CCD with a mask covering every second row of pixels. The three cross-sections were made at two phases, which are 180° appart, and thus show a whole cycle of the modulator. Note how the charges are moved back and forth. Such a choice of geometry is necessary for large CCDs. However, for small CCDs it is possible to screen instead only a single continuous portion of the CCD, having the same size as the unscreened area. The limits on CCD size for this second, preferable, solution are set by the requirement that all the changes must be transferred from the screened to the uncovered part of the CCD within a fraction of the modulation cycle.

The second method of demodulation is normally to be preferred whenever CCDs with the required charge transfer architecture are available. It is simpler, much smaller and lighter, and has recently been applied with great success to solar observations (Povel et al. 1991). It is free from noise that could arise from flat–fielding or image matching. Although half of the light is lost if every second pixel row is screened, its polarimetric efficiency can be shown to be as good as that of the first method. If only one contiguous part of the detector needs to be screened, then there is no loss of light (the loss of half the number of pixels, then only leads to a reduced field-of-view), and the second method is superiour in every respect.

In the infrared, CCDs with the necessary charge transfer architecture for the second scheme to work are not yet available. For this wavelength range the first scheme has to be used.

Under–sampling and the use of higher order aliases to achieve high time resolution works the same with two–dimensional detector arrays as with single–channel systems.

4. LIMITATIONS IN ARRAY SIZE

The limitation of the possible array size does not come from the polarimetric use, but from the requirement that the FTS sampling rate has to be relatively high (of the order of kHz) to allow a high time resolution (10 sec) without too serious compromises of the allowed spectral band width (the alias order should not be excessively large). If one uses CCD–type detectors, their read–out rate is limited to typically 5 MHz. This means that with a sampling rate of a few kHz, it is hardly possible to use arrays larger than 32 × 32. For such small arrays it is conceivable that the mask in front of the chip required by the second demodulation scheme is chosen such that 32 consecutive rows are covered or left uncovered. In this manner the second, more elegant, scheme may be used without any loss of light.

Another problem is that each read–out generates considerable read–out noise, which may drown the tiny polarization signal unless it can be greatly suppressed. Such suppression is possible by using the technique of "double correlated sampling" of the CCD (White et al. 1974; Livingston et al. 1976). Thermal noise is suppressed by cooling the detector. These problems are not specific to polarimetry, but will be encountered for any type of imaging spectrometer with a large spectral coverage.

Although the detector size may thus be limited to about 32 × 32 pixels, one should keep in mind that each of these 1 000 pixels provides a high–resolution spectrum in each of the four Stokes parameters. The information content is thus enormous and puts great demands on the computer data handling system to be used.

REFERENCES

Brault, J.W.: 1978, *Osserv. Mem. Oss. Astrofis. Arcetri* **106**, 33

Livingston, W.C., Harvey, J., Slaughter, C., Trumbo, D.: 1976, *Appl. Opt.* **15**, 40.

Povel, H., Aebersold, H., Stenflo, J.O.: 1990, *Appl. Opt.* **29**, 1186.

Povel, H., Keller, C.U., Stenflo, J.O.: 1991, in *Solar Polarimetry*, L.J. November (Ed.), National Solar Obs., Sunspot, NM, p. 102 Modulators.

Solanki, S.K.: 1987, in *The Role of Fine-Scale Magnetic Fields on the Structure of the Solar Atmosphere*, eds. E.H. Schröter, M. Vázquez, A.A. Wyller, Cambridge University Press, Cambridge, p.67.

Solanki, S.K., Stenflo, J.O.: 1986, *Astron. Astrophys.* **170**, 120

Stenflo, J.O.: 1989, *Astron.Astrophys.Rev.* **I**, 3.

Stenflo, J.O., Solanki, S.K., Harvey, J.W.: 1987, *Astron.Astrophys.* **171**, 305.

Stenflo, J.O., Povel, H.: 1985, *Appl. Opt.* **24**, 3893.

Stenflo, J.O., Harvey, J.W., Brault, J.W., Solanki, S.: 1984, *Astron. Astrophys.* **131**, 333.

Stenflo, J.O., Twerenbold, D., Harvey, J.W., Brault, J.W.: 1983, *Astron. Astrophys. Suppl. Ser.* **54**, 505.

White, M.H., Lampe, D.R., Blaha, F.C., Mack, I.A.: 1974, *IEEE J. Solid–State Circuits* **SC–9**, 1.